New ferroelectric: Bis-thiourea pyridinium bromide inclusion compound

Piotr Czarnecki and Aleksandra Pajzderska
Faculty of Physics, Adam Mickiewicz University, 61-614 Poznan, Poland

Eric Collet and Loic Toupet
Université de Rennes 1, Institut de Physique de Rennes, UMR UR1-CNRS 6251, F-35000 Rennes, France

Jan Wąsicki[a)]
Faculty of Physics, Adam Mickiewicz University, 61-614 Poznan, Poland

(Received 9 May 2012; accepted 21 August 2012)

Dielectric measurements (permittivity and hysteresis loop) of monocrystals of bis-thiourea pyridinium bromide inclusion compound have revealed for the first time ferroelectric properties of the studied samples. In the present article, a model of ferroelectric ordering on the basis of single-crystal x-ray diffraction data is described. In the low-temperature phase, the spontaneous polarization is directed along the *a* axis and ferroelectricity is of the mixed type (displacement and order-disorder component), whereas in the intermediate phase the spontaneous polarization is directed along the *c* axis and ferroelectricity is of the order-disorder type.

I. INTRODUCTION

Intensive search for new ferroelectric materials is of continued interest for both pure theoretical research and practical application thereof.[1,2] As yet, mainly the inorganic ferroelectric materials have found important applications but the search for organic ones is expected to bring interesting materials for future applications in electronics as nanodevices.[3,4] Extensive research has also been focused on understanding the origin of spontaneous polarization after detailed crystalline structure of ferroelectric phases had been determined.[5–8]

One group of the known and widely studied organic ferroelectric materials is the pyridinium salts: pyridinium tetrafluoroborate [(PyH)BF_4], pyridinium perchlorate [(PyH)ClO_4], pyridinium perrhenate [(PyH)ReO_4], pyridinium periodate [(PyH)IO_4], pyridinium fluorosulfonate [(PyH)FSO_3], pyridinium fluorochromate [(PyH)$FCrO_3$].[9–20] In these salts at room temperature the pyridinium cations are disordered and on decreasing temperature their ordering increases in a sequence of two or more phase transitions. The pyridinium cation has a dipole moment and the process of it's ordering is accompanied by the appearance of ferroelectric phases. Of key importance in the studies of the nature of ferroelectricity is analysis of dynamics of the pyridinium cations and determination of the structural conditions of the appearance of spontaneous polarization.[21–23] The ferroelectric pyridinium salts were classified as order-disorder type materials.[22,24,25] However, the ferroelectric properties were not found in the halide pyridinium salts with spherical anions as with iodide, bromide, and chloride because of the antiparallel ordering of pyridinium cations.

An interesting study was performed with pyridinium salts confined in the rigid entrapment made of thiourea molecules as a host sublattice. So far four such systems are known with the chloride, bromide, iodide, and nitrate anions, hereafter denoted as inclusion compounds of bis-thiourea pyridinium chloride (T_2(PyH)Cl), bis-thiourea pyridinium bromide (T_2(PyH)Br), bis-thiourea pyridinium iodide (T_2(PyH)I), and bis-thiourea pyridinium nitrate (T_2(PyH)NO_3), respectively.[26–28] In the first three systems the anion is spherical, whereas in the fourth—it is planar. These compounds have been intensively studied as to their structural,[27,29] dynamic,[30–38] and possibly ferroelectric properties.[27,29,39] Research of ferroelectric properties in the family of thiourea pyridinium salts inclusion compounds with pyridinium salts are important because, to the best of our knowledge, other thiourea inclusion complexes with organic molecules as guest are not ferroelectric materials. Recently, ferroelectric properties have been found in the low-temperature and intermediate phases of bis-thiourea pyridinium iodide inclusion compound [T_2(PyH)I] and in the low-temperature phase of bis-thiourea pyridinium nitrate inclusion compound [T_2(PyH)NO_3].[27] However, it should be emphasized that the hysteresis loop evidencing the ferroelectric character was recorded only for the low-temperature phase of bis-thiourea pyridinium iodide. A detailed analysis of the structural data has permitted to propose a model of ferroelectricity in these compounds. The ferroelectricity was found to be related with the ordering of the pyridinium cation and with the

[a)]Address all correspondence to this author.
e-mail: jwasicki@amu.edu.pl
DOI: 10.1557/jmr.2012.301

 © Materials Research Society 2012

https://doi.org/10.1557/jmr.2012.301 Published online by Cambridge University Press

asymmetric mutual displacement of the ions.[39] The search for ferroelectricity in the third compound belonging to this family bis-thiourea pyridinium chloride inclusion compound T_2(PyH)Cl, of the polar intermediate phase ($Cmc2_1$) has failed.[28] However, this result should not be treated as final as the experiment was performed on polycrystalline samples. The question that we would like to consider here is whether another compound from this group, namely bis-thiourea pyridinium bromide inclusion compound T_2(PyH)Br, shows ferroelectric properties, which seems possible as the space group of its low-temperature phase ($P2_1cn$) is the same as that of bis-thiourea pyridinium iodide inclusion compound T_2(PyH)I known to show such properties. The first reports on the structure of T_2(PyH)Br at room temperature can be found in Ref. 40. Prout et al.[26] gave estimated phase transition temperatures and x-ray diffraction (XRD) data for the three phases of T_2(PyH)Br at 100, 150, and 295 K. The measurements were made for partially deuterated samples. Differential scanning calorimetry (DSC) measurements determined the phase transition temperatures 180 K and 150/152 K on cooling/heating[36] for protonated samples. Preliminary dielectric studies of this compound were made for polycrystalline samples[36] as the attempts at growing adequate size monocrystals failed. For the polycrystalline samples no electric hysteresis loops, proving ferroelectric properties, were observed.

The present article reports new results of a dielectric study of T_2(PyH)Br monocrystals, revealing ferroelectric properties of this material. On the basis of XRD study we propose a model of ferroelectricity ordering in this compound. The structural measurements were performed at 10, 100, 158, 200 K for protonated samples, in contrast to those presented in Ref. 26. Reinvestigation was necessary as the structure of the intermediate phase presented earlier was determined exactly at the phase transition temperature.

II. EXPERIMENTAL

The inclusion compound of bis-thiourea pyridinium bromide (T_2(PyH)Br) was synthesized by the method described in Ref. 26. The needle-like monocrystals obtained were of about 30 mm in length and 0.2 × 0.1 mm in cross section. The monocrystals were oriented by the x-ray method and the long axis of the needle was the *c* direction. Dielectric measurements were made along the directions *c* ([001]) and *a* ([100]) for small monocrystals. Because of the small size of the crystals, several oriented crystals were stacked to increase the area for the measurements along the *c* direction. The area of the samples perpendicular to the *c* direction was ~0.2 mm^2. The measurements along *a* direction were performed on the single small monocrystals of a thickness 0.1–0.2 mm and the area of ~0.6 mm^2. The (100) and (001) faces of the samples were covered with sputtered gold electrodes.

Permittivity was measured by Hewlett-Packard 4192 Impedance Analyzer (Yokogava- Hewlett Packard Ltd., Tokyo, Japan) for 63 kHz in the temperature range of 110–250 K with the cooling rate 0.1/0.5 (K/min) close and far from the phase transition temperatures respectively. The hysteresis loop was recorded by Keithley 6517B electrometer (Keithley Instruments, Inc., Cleveland, OH).

XRD studies were performed on single crystals with typical sizes around 0.150 × 0.250 × 0.400 mm^3. The diffraction experiments were carried out on a Xcalibur 3 four-circle diffractometer (Oxford Diffraction) equipped with a 2D sapphire 3 CCD detector with Mo K_α radiation (λ = 0.71069 Å). The unit cell parameters and the data reduction were obtained with CrysAlis software from Oxford Diffraction. The structures were solved with SIR-97 and refined with SHELXL97. Results of the structure refinement at 200 K (CCDC 842394), 158 (CCDC 842395), 100 K (CCDC 842388), and 10 K (CCDC 842397) gave final *R* factor $0.0237 < R < 0.0366$, as presented in Table I. The single crystals were mounted in an Oxford Cryosystems nitrogen-flow cryostat for measurements down to 80 K, with a temperature stability of 0.1 K. An Oxford Diffraction Helijet helium-flow cryostat was used to collect structural data at 10 K.

TABLE I. Crystal data and structure refinement measured at 200, 158, 100, and 10 K (CCDC reference numbers are: 842394, 842395, 842388, 842397, respectively).

Temperature	200 K	158 K	100 K	10 K
Empirical formula	$C_7 H_{13} Br N_5 S_2$			
Formula weight	311.25			
Crystal system	Orthorhombic			
Space group	*Cmcm*	$Cmc2_1$	$P2_1cn$	$P2_1cn$
a (Å)	14.733(4)	44.005(7)	14.431(3)	14.3323(9)
b (Å)	10.840(3)	10.792(1)	10.999(2)	10.9617(6)
c (Å)	8.355(2)	8.345(1)	8.297(1)	8.2808(5)
V (Å^3)	1334.3(6)	3963.1(9)	1317.0(4)	1300.97(13)
Z	4	12	4	4
Density (calc.) (g/cm^3)	1.614	1.565	1.570	1.589
Absorption coefficient (mm^{-1})	3.378	3.407	3.417	3.459
F(000)	652	1884	628	628
θ range (°)	3.76→26.97	3.70→27.0	3.70→27.0	2.84→26.99
Collected data	15800	45938	30271	8753
Unique data	809	4386	2880	2741
R_{int}	0.055	0.046	0.0601	0.0354
Data/restraints/ parameters	809/0/42	4386/1/209	2880/1/136	2741/1/136
Goodness-of-fit on F^2	1.083	0.920	1.080	1.021
*R*1 [$I > 2\sigma(I)$]	0.0237	0.0274	0.0366	0.0366
*wR*2 [$I > 2\sigma(I)$]	0.0624	0.0685	0.1036	0.0913
*R*1 (all data)	0.0266	0.0539	0.0462	0.498
*wR*2 (all data)	0.0636	0.0738	0.1064	0.0943

https://doi.org/10.1557/jmr.2012.301 Published online by Cambridge University Press

III. RESULTS

A. Single-crystal XRD

Prout et al.[26] previously reported, using XRD data, the existence of three structural phases of different symmetries, which are reinvestigated here. The first one existing at high temperature (HT) is observed above 180 K and corresponds to the high-symmetry phase with *Cmcm* space group (CCDC 842394). At 200 K the corresponding lattice parameters are $a_{HT} = 14.73$ Å, $b_{HT} = 10.84$ Å, $c_{HT} = 8.35$ Å. Four hydrogen-bonded thiourea ribbons, equivalent by symmetry, form a channel parallel to the *c* axis with an approximately square cross section (Fig. 1). In each channel pyridinium cations are stacked. In the high-symmetry HT phase, the position of the nitrogen atoms of the pyridinium cations are disordered as the molecule is located on inversion symmetry site and on two mirrors (Fig. 2). There are two channels per unit cell, which are equivalent by symmetry (C lattice).

In the 180–150 range, an intermediate phase appears, with space group $Cmc2_1$, and at 158 K the corresponding lattice parameters are $a_{INT} = 44.01$ Å, $b_{INT} = 10.79$ Å, $c_{INT} = 8.35$ Å, indicating a triplication of the *a* axis (Fig. 3) with respect to the high-temperature phase ($a_{INT} = 3\ a_{HT}$). The associated structural reorganization is very similar to the ones observed for the chloride compound.[28] The three channels existing in the tripled unit cell split into two types. For one of them, equivalent by symmetry, the mirror symmetry perpendicular to *a* axis on which pyridinium cations are located is kept, involving an ordering of the N atoms of the cations in this plane. For the two others, the mirror symmetry is lost and the N atoms move out of the Wickoff position mentioned above. As a result of the symmetry breaking, a polar axis along *c* appears.

Below 150 K, a low-temperature (LT) phase appears, with space group $P2_1cn$, and at 100 K the corresponding lattice parameters are $a_{LT} = 14.43$ Å, $b_{LT} = 10.99$ Å, $c_{LT} = 8.30$ Å. In this phase (Fig. 4), all the channels are equivalent but there are now two independent thiourea

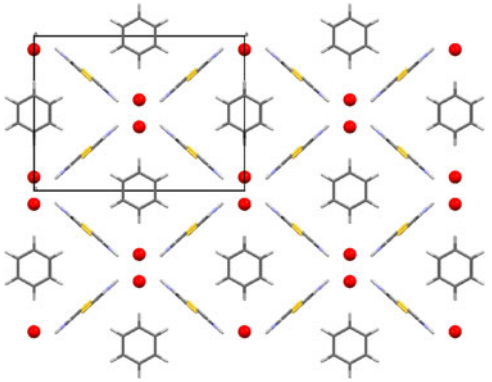


FIG. 1. Projection of the structure of the high-temperature phase of T_2(PyH)Br along *c* axis (in the *ab* plane). Nitrogen atom of the pyridinium cation is disordered.

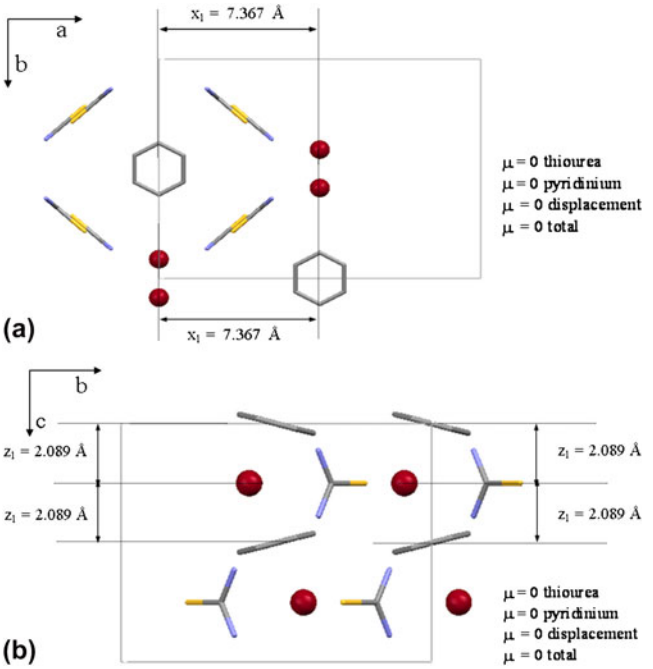


FIG. 2. Molecular arrangement in the high-temperature phase of T_2(PyH)Br (a) along *c* axis (in the *ab* plane), (b) along *a* axis (in the *bc* plane). The resultant dipole moment is equal to zero.

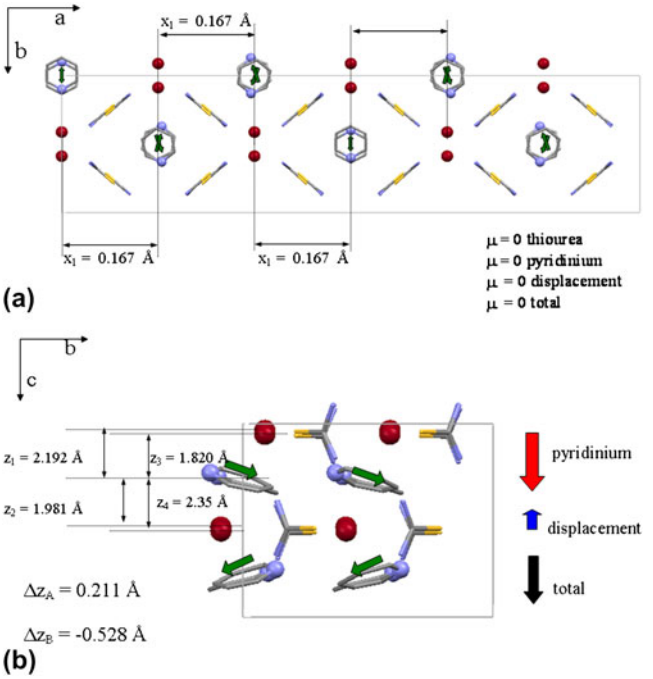


FIG. 3. Molecular arrangement in the intermediate temperature phase of T_2(PyH)Br (a) along *c* axis (in the *ab* plane), (b) along *a* axis (in the *bc* plane). The arrows indicate the resultant dipolar moment of the cations in the elementary cell. The arrows on the right-hand side of the figure indicate the resultant dipolar moment of all of the cations, the dipolar moment originating from the mutual shift of the ions, and the total dipolar moment. The resultant dipole moment is observed only in *c* direction.

https://doi.org/10.1557/jmr.2012.301 Published online by Cambridge University Press

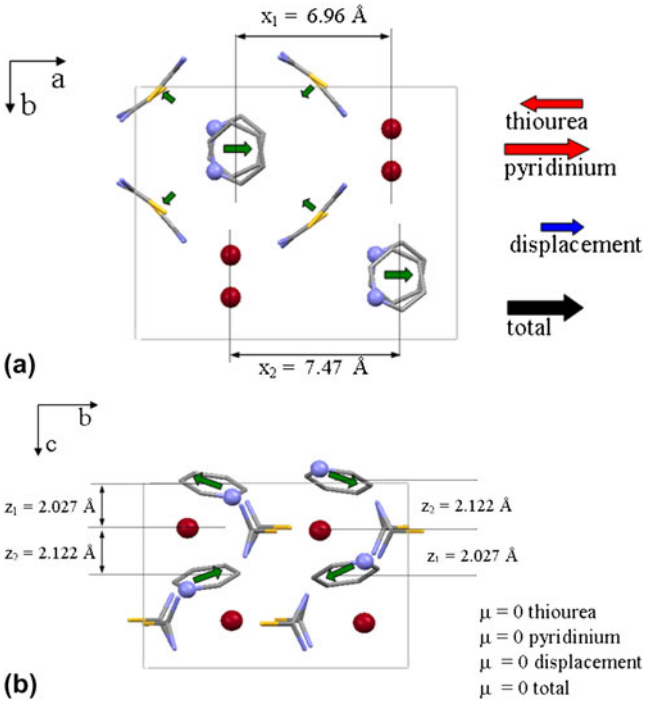


FIG. 4. Molecular arrangement in the low-temperature phase of T_2(PyH)Br (a) along *c* axis (in the *ab* plane), (b) along *a* axis (in the *bc* plane). The arrows indicate the resultant dipolar moment of individual ribbons of thiourea molecules and that of the pyridinium cations in the elementary cell. The arrows on the right-hand side of the figure indicate the resultant dipolar moment of all of the ribbons of thiourea molecules and all of the cations, the dipolar moment originating from the mutual shift of the ions, and the total dipolar moment. The resultant dipole moment is observed only in *a* direction.

molecules in the unit cell (tilted with respect to the HT phase), and the symmetry breaking is associated with a tilting of the pyridinium cations and an ordering of the N positions. In this phase, *a* becomes the polar axis.

B. Dielectric measurements

Results of permittivity measurements along the *c* and *a* directions are presented in Fig. 5 and reveal a clear anisotropy of permittivity in these two directions. In the *c* direction there is a ferroelectric-like anomaly at $T_1^{p.t.} = 180$ K. In the *a* direction an anomaly at temperature $T_1^{p.t.} = 180$ K, is hardly seen but at temperature $T_2^{p.t.} = 154$ K there is a distinct discontinuous change in permittivity related to discontinuous phase transition toward the low-temperature phase. For this phase transition, the thermal hysteresis (about 5 K on heating/cooling) is observed which is typical of discontinuous phase transitions.

The clearly seen anisotropy in permittivity along the *a* and *c* directions is related to the structural changes at temperatures $T_1^{p.t.}$ and $T_2^{p.t.}$. At temperature $T_1^{p.t.}$, the crystal symmetry changes from *Cmcm* to $Cmc2_1$ as a consequence of the appearance of the polar axis in the *c* direction. This type of phase transition is ferroelectric. Moreover, the elementary cell dimension in the *a* direction is 3-fold increased. The ferroelectric phase transitions accompanied with a 3-fold increase in the elementary cell are not often observed. However, such a phase transition has been detected recently in the hexagonal system for inorganic compounds.[5,41,42] In T_2(PyH)Br such a phase transition with a 3-fold increase in the elementary cell takes place in the orthorhombic system and is related to partial ordering of the pyridinium cation at $T_1^{p.t.} = 180$ K. In the intermediate phase it was impossible to observe an electric hysteresis loop, which was probably related to a very small area of the monocrystal in the plane (110) (bc plane)—nearly 0.2 mm^2—and a low spontaneous polarization (which will be discussed below). The maximum permittivity at temperature $T_1^{p.t.}$ reaches over 100 and points to a ferroelectric phase transition.

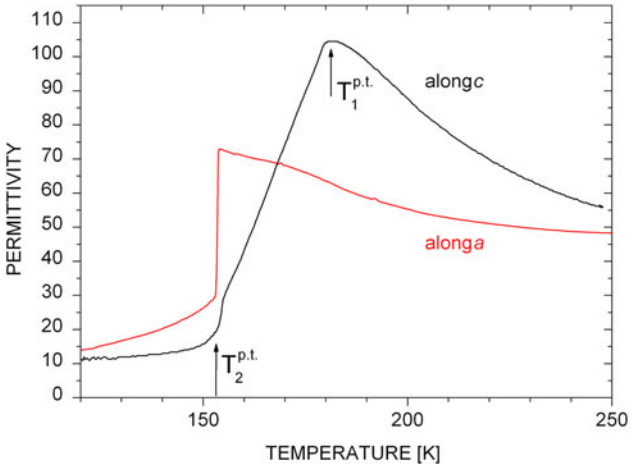


FIG. 5. Permittivity dependence on temperature measured along the *a* and *c* axes (cooling).

At the discontinuous phase transition at $T_2^{p.t.}$ the crystal symmetry changes from $Cmc2_1$ to $P2_1cn$, which is accompanied by a change in the direction of the polar axis by 90°; the polar axis becomes the *a* direction. In the LT phase an electric hysteresis loop (Fig. 6) was observed for measurements in the *a* direction.

This occurrence of an electric hysteresis loop is the experimental evidence that bis-thiourea pyridinium bromide inclusion compound [T_2(PyH)Br] is a new ferroelectric. The loop was observed in the vicinity of the phase transition temperature below $T_2^{p.t.}$. With decreasing temperature in the LT phase a fast increase in the coercive field was noted and for this reason the loop was unsaturated. The estimated value of spontaneous polarization of 0.55 μC/cm^2 is charged with an error of about 30% because of the uncertainty of area measurement in such a small crystal. Above temperature $T_2^{p.t.}$, the spontaneous polarization discontinuously disappears as expected for a first order transition.

The crystal T_2(PyH)Br is the second bis-thiourea pyridinium salts inclusion compound confirmed to show

https://doi.org/10.1557/jmr.2012.301 Published online by Cambridge University Press

ferroelectric properties by electric hysteresis loop observation. A similar observation was made for T_2(PyH)I,[29] but no hysteresis loop was recorded and it is also the case for T_2PyNO_3[27] although the observed dielectric anomaly and change in the crystalline structure suggest a ferroelectric transition.

The hitherto studied bis-thiourea pyridinium salts inclusion compound[26] are isostructural in the high-temperature disordered phases (*Cmcm*), but show different sequences of phase transitions leading to the ordered low-temperature phases. In T_2(PyH)Br, the change from the centrosymmetric phase *Cmcm* at temperature $T_1^{p.t.}$ to the polar phase $Cmc2_1$ accompanied with a 3-fold extension of the elementary cell is continuous, similar to that in T_2(PyH)Cl[28] and ferroelectric. The phase transition at temperature $T_2^{p.t.}$ in bis-thiourea pyridinium bromide inclusion compound T_2(PyH)Br is discontinuous and leads to the ferroelectric phase with the polarization vector directed along the *a* axis, whereas in bis-thiourea pyridinium chloride inclusion compound T_2(PyH)Cl the transition at temperature $T_2^{p.t.}$ is continuous and leads to the centrosymmetric phase Pbca. In bis-thiourea pyridinium iodide inclusion compound T_2(PyH)I the sequence of reaching the ordered phase is as follows $Cmcm \rightarrow C2mc \rightarrow P2_1nc$. The low-temperature phase of T_2(PyH)I is similar to that of T_2(PyH)Br, but in the ferroelectric intermediate phase *C2mc* the 3-fold extension of the elementary cell does not take place.

IV. THE MODEL OF FERROELECTRICITY

The dielectric study results presented above prove the ferroelectric properties of this system. The structural data obtained by XRD permit the proposal of a model of ferroelectricity.

It should be remembered that both the thiourea molecules and the pyridinium cations are endowed with the dipole moments. The thiourea molecules are linked via the hydrogen bonds N-H....S and arranged in the head-to-tail mode making a ribbon along the z axis. The flat ribbon does not have a resultant dipole moment in contrast with the bent ribbon, which has such a resultant dipole moment perpendicular to its plane determined by the heavy atoms.[39]

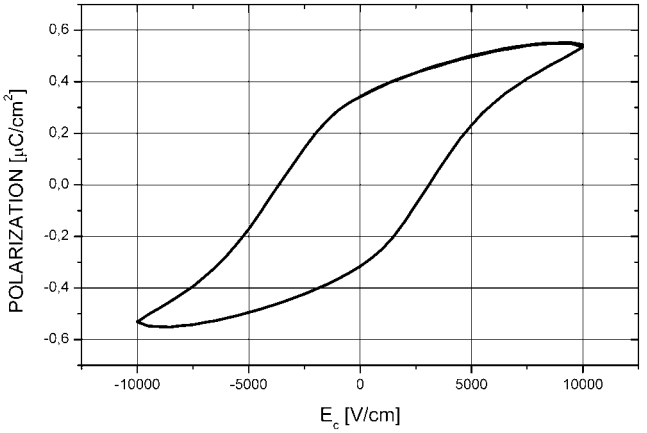


FIG. 6. Hysteresis loop recorded at 152 K (low-temperature phase) in the *a* direction.

Analysis of the contributions of the dipole moments coming from the thiourea ribbons, pyridinium cations and relative displacement of the cations and anions in T_2(PyH)Br was performed in the same way as for T_2(PyH)I and T_2(PyH)NO_3.[39] As in our earlier work, for quantitative evaluation of the components of the dipole moments in individual phases, we have assumed the dipole moment of thiourea molecule as 6.5 D, while that of the pyridinium cation as 2 D. The calculated resultant dipole moments and their values expressed in terms of polarization (taking into account the elementary cell volume) are given in Table II.

Figures 2–4 present the projections of the elementary cell of T_2(PyH)Br in three phases onto the (*a*, *b*) and (*b*, *c*) planes, marking the dipole moments of the pyridinium cations, thiourea ribbons and those following from relative displacement of the ions.

In the LT phase of T_2(PyH)Br the resultant dipole moment from the four nonplanar ribbons of thiourea present in the elementary cell is directed along the *a* axis [Fig. 4(a)], whereas the resultant dipole moment from the four cations is directed in the opposite direction ($-a$). The dipole moment originating from the mutual displacement of the anion and cation is also directed along the $-a$ axis. Figure 4 presents the distances between the centers of the nearest anions and cations along the *a* axis (denoted by x_1 and x_2, respectively). These distances differ by $\Delta x = x_1 - x_2 = 0.51$ Å (at 100 K). In this phase, the contributions brought by the dipole moments from the cations and thiourea ribbons along the *a* axis are almost compensated and thus, the resultant dipolar moment and resultant polarization of the elementary cell is determined mainly by the mutual displacement of the cations and anions. The obtained value of polarization of 1 μC/cm^2 is comparable with that found for T_2(PyH)I and T_2(PyH)NO_3. It should be emphasized that no resultant dipole moment is observed along the *c* axis [Fig. 4(b)] as the projections of the dipole moments from pyridinium cations and those from the mutual ion displacement are fully compensated.

TABLE II. The spontaneous polarization of the elementary cell of T_2(PyH)Br along *a* and *c* axis.

	Polarization (μC/cm^2) (calculated values)					
	Along *a* axis			Along *c* axis		
	LT	INT	HT	LT	INT	HT
Thiourea	1.04	0	0	0	0	0
Pyridinium cation	−1.45	0	0	0	0.49	0
Displacive	−0.63	0	0	0	−0.09	0
Total	−1.04	0	0	0	0.40	0

https://doi.org/10.1557/jmr.2012.301 Published online by Cambridge University Press

In INT phase [Figs. 3(a) and 3(b)] the analysis is more difficult because of the 3-fold extension of the elementary cell along the *a* axis. The resultant dipole moment along the *a* axis [Fig. 3(a)] is zero. The thiourea ribbons are planar and give zero contribution, whereas the projections of the dipole moments of the cations are compensated and the distances between the centers of the nearest cations and anions in the elementary cell are the same. In this phase, the resultant dipole moment comes from pyridinium cations and it is directed along the *c* axis. Also, the contribution to the resultant dipole moment from the displacement of the centers of gravity of the anions relative to those of the cations is in the same direction. As in the intermediate phase, there are two types of crystallographically inequivalent pyridinium ions, *A* and *B* and two types of bromide anions, the relative cation-anion displacements are different and in Fig. 3(b) they are marked as $\Delta z_A = 0.211$ Å and $\Delta z_B = -0.528$ Å. In the elementary cell, there are twice as many cations and anions of type A than those of type B, so the distance Δz_A is taken twice. The two displacements have the opposite senses so the contribution due to the displacement is small. Consequently, in this phase, in contrast to LT phase [also to T_2(PyH)I and T_2(PyH)NO_3], the main contribution to the resultant dipole moment comes from pyridinium ions and the estimated polarization is about twice smaller than in LT phase. The cation dipole moments show a ferroelectric ordering. A characteristic feature of this phase is the contribution of dipole moments of the molecules at different site symmetry in the net polarization.

In HT phase no resultant dipole moment is observed along the *a* or *c* axes (Fig. 2). The thiourea molecule ribbons are planar and their contribution to the resultant dipole moment along the *a* direction is zero. The dipole moment of the cations is averaged to zero as disordered cations are located on inversion symmetry site, resulting from reorientation along the axis perpendicular to their plane, through inequivalent potential energy wells.[32] As the distances between the centers of the nearest cations and anions are the same, $\Delta x = 0$ and there is no contribution resulting from the ion displacement. Along the *c* axis the displacements $\Delta z = 0.095$ Å are compensated by symmetry.

As can be seen from the above-mentioned discussions, the models of ferroelectricity in the low-temperature and intermediate phases are different. In the INT phase the polarization is a result of the dipole moments of the pyridinium cations and appears along the *c* axis, whereas in the LT phase, the polarization is a result of the contributions of the cation dipole moments and relative displacement of the ions. Thus, in the INT phase the compound studied is a ferroelectric of order-disorder type, whereas in the LT phase it is a mixed type ferroelectric of both displacement and order-disorder characters.

V. CONCLUSIONS

From the results presented and discussed above, one can draw the following conclusions regarding the ferroelectric phase transitions in T_2(PyH)Br. The structural studies have confirmed the sequence of phase transitions from high-temperature to low-temperature phases $Cmcm \rightarrow Cmc2_1 \rightarrow P2_1cn$ already reported in the literature,[11] whereas no phase transition was found in the range from 10 to 100 K. In the intermediate phase the 3-fold extension of the elementary cell along the *a* axis is observed and the positions of nitrogen atoms in pyridinium cations have been accurately determined in the present work. Our dielectric study for the *c* and *a* directions, performed on very small monocrystals, has revealed a significant anisotropy of permittivity and a hysteresis loop in the low-temperature phase of the crystal along the *a* axis, proving the ferroelectric ordering in T_2(PyH)Br in this phase. The first-order character of the phase transition from LT- to INT phase revealed by dielectric studies suggests that T_2(PyH)Br is also ferroelectrically ordered in the INT phase. By combining structural and ferroelectric studies we have proposed a model of ferroelectricity in T_2(PyH)Br, according to which in INT phase the ferroelectric ordering is of order-disorder type (spontaneous polarization along the *c* axis), whereas in LT phase the ferroelectric ordering is of mixed displacement and order-disorder type (spontaneous polarization along the *a* axis).

ACKNOWLEDGMENTS

This work has been partially financed by the Ministry of Science and Higher Education of Poland, Grant No. 202 032937, and supported by Rennes Region Bretagne (CREATE Ultimate 4146).

REFERENCES

1. J.F. Scott: Applications of modern ferroelectrics. *Science* **315**, 954 (2007).
2. C.H. Ahn, K.M. Rabe, and J.M. Triscone: Ferroelectricity at the nanoscale: Local polarization in oxide thin films and heterostructures. *Science* **303**, 488 (2004).
3. S. Horiuchi, Y. Tokunaga, G. Giovannetti, S. Picozzi, H. Itoh, R. Shimano, R. Kumai, and Y. Tokura: Above-room-temperature ferroelectricity in a single-component molecular crystal. *Nature* **463**, 789 (2010).
4. S. Horiuchi, F. Ishii, R. Kumai, Y. Okimoto, H. Tachibana, N. Nagaosa, and T. Yoshinori: Ferroelectricity near room temperature in cocrystals of nonpolar organic molecules. *Nat. Mater.* **4**, 163 (2005).
5. B.B. Van Aken, T.T. Palstra, A. Filippetti, and N.A. Spaldi: The origin of ferroelectricity in magnetoelectric $YMnO_3$. *Nat. Mater.* **3**, 164 (2004).
6. M. Szafrański: Simple guanidinium salts revisited: Room–temperature ferroelectricity in hydrogen-bonded supramolecular structures. *J. Phys. Chem. B* **115**, 8755 (2011).
7. A. Katrusiak and M. Szafrański: Ferroelectricity in NH...N hydrogen bonded crystals. *Phys. Rev. Lett.* **82**, 576 (1999).

https://doi.org/10.1557/jmr.2012.301 Published online by Cambridge University Press

8. M. Szafranski and M. Jarek: From nonpolar to ferroelectric crystal structure: The temperature-tuned growth of two guanidinium ethoxysulfonate polymorphs. *J. Phys. Chem. B* **112**, 3101 (2008).
9. P. Czarnecki, W. Nawrocik, Z. Pajak, and J. Wasicki: Ferroelectric properties of pyridinium tetrafluoroborate. *Phys. Rev. B* **49**, 1511 (1994).
10. P. Czarnecki, W. Nawrocik, Z. Pajak, and J. Wasicki: Ferroelectric properties of pyridinium perchlorate. *J. Phys. Condens. Matter* **6**, 4955 (1994).
11. J. Wasicki, P. Czarnecki, Z. Pajak, W. Nawrocik, and W. Szczepański: Ferroelectric properties of pyridinium perrhenate. *J. Chem. Phys.* **107**, 576 (1997).
12. Z. Pajak, P. Czarnecki, J. Wasicki, and W. Nawrocik: Ferroelectric properties of pyridinium periodate. *J. Chem. Phys.* **109**, 6420 (1998).
13. H. Maluszynska, P. Czarnecki, S. Lewicki, J. Wasicki, and M. Daniec: Structure and dynamics of ferroelectric pyridinium periodate. *J. Phys. Condens. Matter* **13**, 11053 (2001).
14. L. Bobrowicz-Sarga, P. Czarnecki, S. Lewicki, I. Natkaniec, W. Nawrocik, and J. Wasicki: Phase transitions in ferroelectric pyridinium periodide under high pressure. *Phase Transitions* **80**, 725 (2007).
15. Z. Pajak, P. Czarnecki, H. Maluszynska, B. Szafranska, and M. Szafran: Ferroelectric properties of pyridinium fluorosulfonate. *J. Chem. Phys.* **113**, 848 (2000).
16. Z. Pajak, H. Maluszynska, and P. Czarnecki: Crystal structure, molecular dynamics, and polar properties of pyridinium fluorochromate. *J. Chem. Phys.* **117**, 5303 (2002).
17. J. Przesławski, J. Jamiński, and Z. Czapla. Specific heat anomalies in ferroelectric $PyBF_4$. *Ferroelectrics* **363**, 64 (2008).
18. J. Hatori, M. Komukae, Z. Czapla, and T. Osaka: Dielectric dispersion studies in pyridinium periodate single crystal. *J. Phys. Soc. Jpn.* **71**, 1431 (2002).
19. M. Hanaya, H. Shibazaki, M. Oguni, T. Nemoto, and Y. Ohashi: Orientational ordering/disordering of ions accompanied by phase transitions in pyridinium tetrafluoroborate crystal. *J. Phys. Chem. Solids* **61**, 651 (2000).
20. B. Beck, K. Muller, and E. Roduner: ^{2}H NMR study of dynamics, ordering, and phase transitions in ferroelectric pyridinium tetrafluoroborate. *Chem. Mater.* **15**, 1739 (2003).
21. J. Józków, R. Jakubas, and J. Baran: Infrared investigation of the order–disorder phase transitions in $(C_5H_5NH)_6Bi_4Cl_{18}$. *J. Mol. Struct.* **555**, 273 (2000).
22. J. Wasicki, A. Pajzderska, and Z. Fojud: Temperature dependence of spontaneous polarization in order−disorder pyridinium periodate extracted from ^{2}H NMR data. *J. Phys. Chem. C* **112**, 7503 (2008).
23. J. Jozkow, W. Medycki, J. Zaleski, R. Jakubas, G. Bator, and Z. Ciunik: Structure, phase transition and molecular motions in $(C_5H_5NH)BiCl_4$. *Phys. Chem. Chem. Phys.* **3**, 3222 (2001).
24. M. Maeda, K. Okada, K. Deguchi, M. Iwata, and I. Suzuki: Dielectric dispersion of pyridinium tetrafluoroborate single crystals. *J. Phys. Soc. Jpn.* **74**, 1416 (2005).
25. M. Hanaya, M. Nomoto, T. Miura, and M. Oguni: Discovery of dipolar-glassy state in a newly found solid–solution system of $C_5NH_6(BF_4)_{1-x}(PF_6)_x$. *Solid State Commun.* **115**, 57 (2000).
26. K. Prout, S.J. Heyes, C.M. Dobson, A. McDaid, T. Maris, M. Muller, and M.J. Seaman: Variable-temperature studies of order/disorder transitions in the thiourea pyridinium halide crystals by XRD and solid-state ^{2}H NMR. *Chem. Mater.* **12**, 3561 (2000).
27. H. Maluszynska and P. Czarnecki: Structure, phase transitions and dielectric properties of a new inclusion compound of bis-thiourea pyridinium nitrate salt. *Z. Kristallogr.* **221**, 218 (2006).
28. A. Pajzderska, J. Wasicki, P. Czarnecki, L. Toupet, and E. Collet: Discovery of an intermediate phase in bis-thiourea pyridinium chloride inclusion compound. *J. Chem. Phys.* **130**, 044503 (2009).
29. H. Maluszynska, P. Czarnecki, Z. Fojud, and J. Wasicki: Redetermination of the structure and dielectric properties of bis(thiourea) pyridinium iodide–a new ferroelectric inclusion compound. *Acta Crystallogr., Sect. B: Struct. Sci.* **64**(5), 572 (2008).
30. A. Pajzderska, M.A. Gonzalez, J.P. Embs, and J. Wasicki: Complex dynamics of pyridinium cation in ferroelectric bis(thiourea)pyridinium iodide studied by quasielastic neutron scattering. *J. Phys. Chem. C* **115**, 15164 (2011).
31. A. Pajzderska, M.A. Gonzalez, and J. Wasicki: Molecular dynamics simulation of cation dynamics in bis-thiourea pyridinium nitrate inclusion compound. *J. Chem. Phys.* **135**, 074508 (2011).
32. A. Pajzderska, M.A. Gonzalez, and J. Wasicki: In-plane pyridinium cation reorientation in bis-thiourea chloride, bromide and iodide: Quasielastic neutron scattering combined with molecular dynamics simulations. *Phys. Chem. Chem. Phys.* **14**, 3949 (2012).
33. M. Grottel, A. Kozak, A. Pajzderska, W. Szczepanski, and J. Wasicki: ^{1}H NMR study of molecular motions in thiourea pyridinium nitrate inclusion compound. *Z. Naturforsch., A* **59**, 505 (2004).
34. M. Grottel, A. Pajzderska, and J. Wasicki: ^{1}H NMR study of molecular motions in thiourea pyridinium halide inclusion compounds. *Z. Naturforsch., A* **58**, 638 (2003).
35. A. Pajzderska, Z. Fojud, R. Goc, and J. Wasicki: Cation dynamics in pyridinium nitrate and bis-thiourea pyridinium nitrate inclusion compound studied by ^{2}H NMR spectroscopy. *J. Phys. Condens. Matter* **19**, 156220 (2007).
36. A. Marczak, P. Czarnecki, and S. Mielcarek: Dielectric spectroscopy of (bis)thiourea pyridinium bromide. *Z. Naturforsch., A* **59**, 857 (2004).
37. A. Pajzderska, M.A. Gonzalez, and J. Wasicki: Quasielastic neutron scattering study of pyridinium cation reorientation in thiourea pyridinium nitrate inclusion compound. *J. Chem. Phys.* **128**, 084507 (2008).
38. A. Pajzderska, P. Czarnecki, J.P. Embs, M.A. Gonzalez, F. Juranyi, J. Krawczyk, B. Peplinska, and J. Wasicki: A study of out-of-plane cation dynamics in a bis-thiourea pyridinium chloride inclusion compound. *Phys. Chem. Chem. Phys.* **13**, 8908 (2011).
39. A. Pajzderska, E. Collet, P. Czarnecki, and J. Wasicki: Ferroelectricity of inclusion compounds of thiourea with pyridinium iodide and nitrate. *J. Phys. Chem. C* **113**, 6282 (2009).
40. M.R. Truter and B.L. Vickery: The crystal structure of bisthiourea pyridinium bromide. *Acta Crystallogr., Sect. B* **28**, 387 (1972).
41. W.K. Lee and H.Z. Cummins: Raman activation of acoustic modes in commensurate A_2BX_4 crystals by zone folding. *Phys. Rev. B* **39**, 4457 (1989).
42. A.S. Gibbs, K.S. Knight, and P. Lightfoot: High-temperature phase transitions of hexagonal $YMnO_3$. *Phys. Rev. B* **83**, 094111 (2011).

https://doi.org/10.1557/jmr.2012.301 Published online by Cambridge University Press